Crystal Engineering Through Particle Size and Shape Measurement, Kinetic Parameter Estimation, Modeling and Control

James B. Rawlings

Department of Chemical and Biological Engineering
University of Wisconsin–Madison

Department of Chemical Engineering
University of South Carolina
10 April 2006

Outline

A brief history...

"Crystal Size Distribution Dynamics, Stability and Control (A Review Paper)," Randolph, 1980.

Technologies do not exist for the on-line instrumental control of CSD.

The literature is rife with theoretical studies of CSD stabilization and/or control, but typically the suggested control variable cannot presently be measured and in no case were any of the control algorithms experimentally investigated.

The current industrial practice of CSD in industrial crystallizers can be summed up in three words: Hold Everything Constant.

A brief history ...10 years later

"Model Identification and Control of Solution Crystallization Processes: A Review," Rawlings, Miller, Witkowski, 1993.

Considerable research effort has been devoted to CSD control, and we are now seeing the advances in measurement and computing technologies necessary for successful industrial implementation.

It is reasonable to expect closed-loop CSD control to become part of accepted industrial practice in the near future.

Measurement technology review

Technique	Description	Reference
Video Microscopy and Image Analysis	• On-line images captured and digitized • Limited to dilute slurries • Shape information present	Patience and Rawlings (2001) Plummer and Kausch (1995) Bharati and MacGregor (1998)
Lasentec particle and vision measurement (PVM)	• In-situ probe coupled with strobing • Numerous images are captured • Dense slurries possible • Randomly oriented particles	Braatz and Hasebe (2001) lasentec.com
Forward laser light scattering	• Energy pattern of scattered light • Ill-conditioned inversion of scattering pattern to CSD	Heffels et al. (1994,1995) Rawlings et al. (1993) www.malvern.co.uk
Transmittance	• In-situ probe • Second moment of CSD • Limited to single scattering	van de Hulst (1981) Matthews and Rawlings (1998) Patience et al. (2001)
Backward laser light scattering Lasentec focused beam reflectance measurement (FBRM)	• In-situ probe • Chord length of CSD • Dense slurries possible	Monnier et al.(1997) lasentec.com
Electro-zone Sensing (Coulter counter)	• Electronically counts particles • Requires a conducting solution • Third moment of CSD	Allen (1997) Rovang and Randolph (1980)

A brief history . . . projecting 10 years in the future

"Tailoring Size, Shape and Composition of the Solid Phase,"
some future researcher, 2010.

A large investment in process technologies required to achieve reliable manufacturing processes for new products in high value-added industries, such as pharmaceuticals, took place in the 1990s. This investment resulted in a revolution in methods for measuring, monitoring, modeling and controlling the creation of the solid phase from solution. All aspects of this formation are now tailored to meet product quality specifications including the size and shape of particles, as well as the multicomponent composition in the solid mixture. It is not clear why the earlier researchers were such pessimists. . .

A systems engineering perspective

- First we need a model...
  - mathematical abstractions of real processes
  - predict behavior over some operating range of interest
- Systems theory can...
  - provide general tools for extracting information from complex models and experimental data
  - examples
    - steady-state analysis
    - parameter estimation
    - optimization
    - on-line estimation and control

Modeling of Populations

Dynamics of populations are determined by applying the equation of continuity.

- Conservation Equation

$$\frac{d}{dt}\int_V f(z,t)d\tau = \int_V (B-D)d\tau$$

$$z = \begin{bmatrix} x \\ y \end{bmatrix} = \begin{bmatrix} \text{external characteristics} \\ \text{internal characteristics} \end{bmatrix}$$

  Assumes that V is large enough to contain a statistically significant portion of the population.

- Microscopic Equation of Continuity

$$\frac{\partial f(z,t)}{\partial t} + \nabla \cdot (f(z,t)v_z) = B - D$$

Application to Crystallization

Population Balance:

$$\frac{\partial f(L,t)}{\partial t} = -G\frac{\partial f(L,t)}{\partial L}$$

in which $f(L,t)$ is the number of crystals of size L at time t, and G is the crystal growth rate.

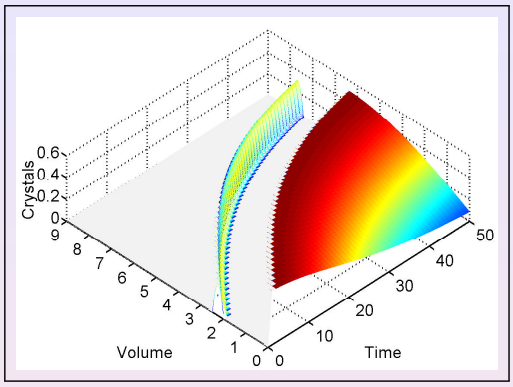

Mass and Energy Balances:

$$\frac{dC}{dt} = -3\rho_c k_v h G\int_0^\infty fL^2 dL \qquad \rho V C_p\frac{dT}{dt} = -3\Delta H_c\rho_c k_v V G\int_0^\infty fL^2 dL - UA(T - T_j(t))$$

Nucleation and Growth in the Bulk:

$$B = k_b\left(\frac{C - C_{sat}(T)}{C_{sat}(T)}\right)^b = k_b S^b \qquad G = k_g\left(\frac{C - C_{sat}(T)}{C_{sat}(T)}\right)^g = k_g S^g$$

A Stochastic Population Balance Alternative

Reaction Mechanism for Nucleation and Growth

$$2M \xrightarrow{k_n} N_1 \qquad \Delta H^n_{\text{rxn}}$$
$$N_n + M \xrightarrow{k_g} N_{n+1} \qquad \Delta H^g_{\text{rxn}}$$

N_n is the number of crystals of size $(n+1)\Delta$ per volume.

Mass Balance

$$M_{\text{tot}} = M_{\text{sat}} + M$$

Energy Balance

$$\frac{dT}{dt} = \frac{UA}{\rho C_p V}(T_j - T)$$

(between reaction events)

Solubility Relationship

$$M_{\text{sat}}(T)$$

Simulating reactions stochastically

- Stochastic kinetic models treat reactions as molecular events
- Consider the well-mixed reaction:

$$A + B \underset{k_{-1}}{\overset{k_1}{\rightleftharpoons}} C$$

$$\begin{bmatrix} A_o \\ B_o \\ C_o \end{bmatrix} = \begin{bmatrix} 10 \\ 50 \\ 0 \end{bmatrix} \text{ molecules}$$

- Scale probabilities by reaction rates
  - $r_1 = k_1 AB$
  - $r_2 = k_{-1} C$
  - $r_{\text{tot}} = r_1 + r_2$

- Randomly select [4, 5, 18]
  1. When the next reaction occurs

$$p(\tau) = r_{\text{tot}} e^{-r_{\text{tot}}\tau}$$

$$\tau = -\frac{\log(p_1)}{r_{\text{tot}}}$$

  2. Which reaction occurs

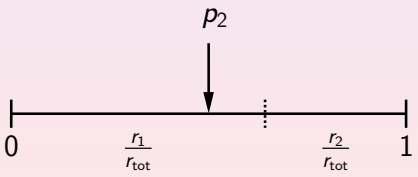

Stochastic Simulation of $A + B \rightleftharpoons C$

One simulation

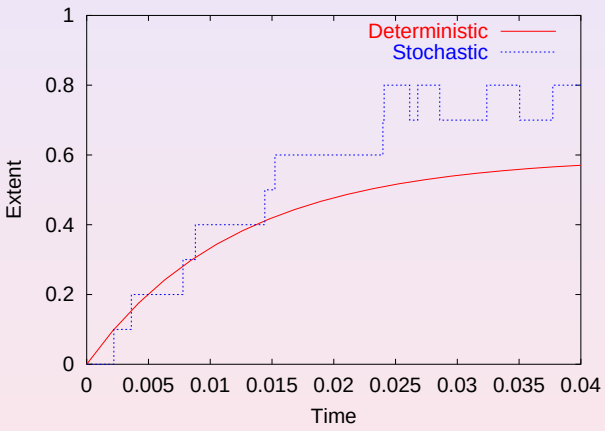

Average of many simulations

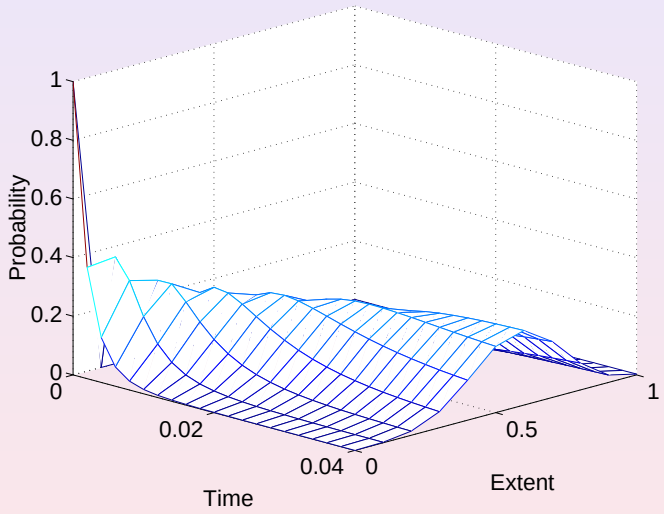

Implications for Crystal Populations

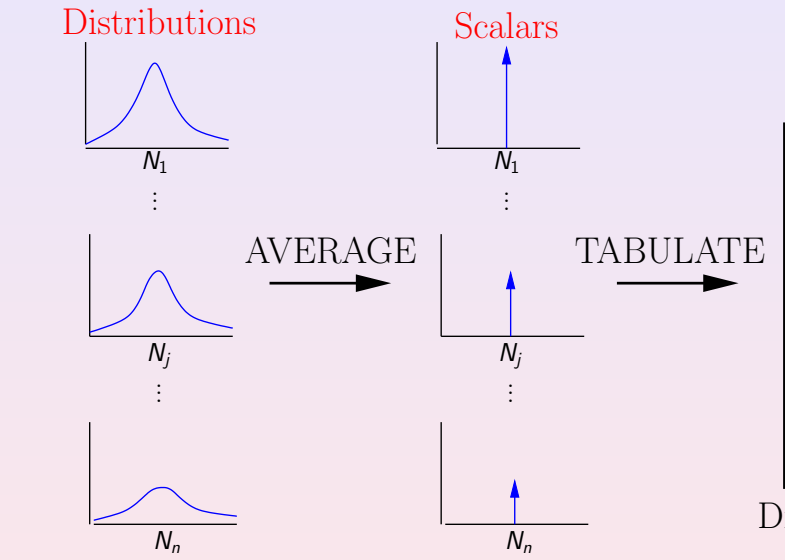

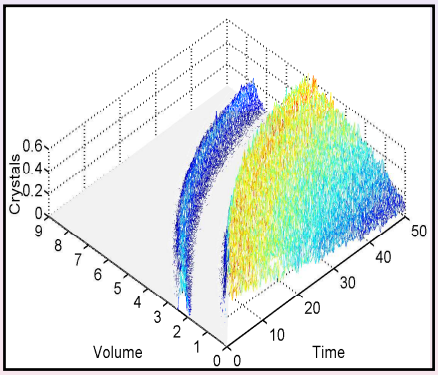

Distribution of Stochastic Averages

Connection to Deterministic Kinetics (Ω = System Size) for $A + B \rightleftharpoons C$

Ω

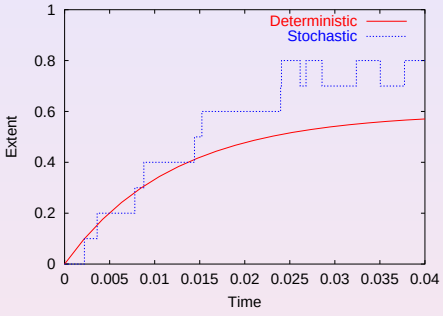

$\Omega \times 10$

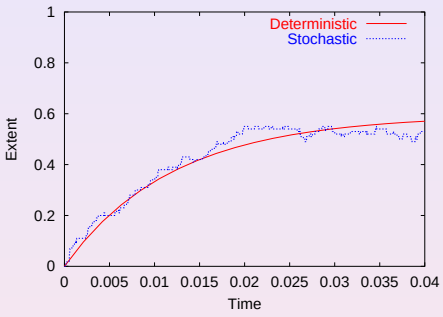

$\Omega \times 100$

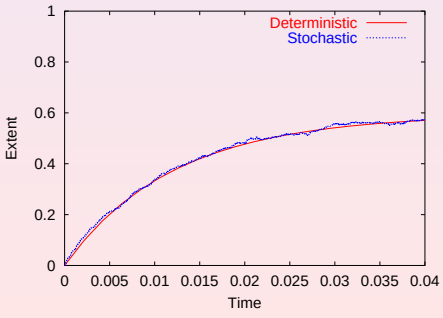

As Ω increases:
Stochastic $\rightarrow$ Deterministic
Computing burden increases!

Stochastic Simulation of Surface Reactions

Reaction Events for CO oxidation

$$\begin{aligned}
\mathrm{CO(g)} + \quad *_\mathrm{i} &\xrightarrow{\alpha} \quad \mathrm{CO}_{*,\mathrm{i}} \\
\mathrm{O_2(g)} + \quad *_\mathrm{i} + \quad *_\mathrm{j} &\xrightarrow{\beta} \quad \mathrm{O}_{*,\mathrm{i}} + \mathrm{O}_{*,\mathrm{j}} \\
\mathrm{CO}_{*,\mathrm{i}} &\xrightarrow{\gamma} \quad \mathrm{CO(g)} + \quad *_\mathrm{i} \\
\mathrm{CO}_{*,\mathrm{i}} + \quad \mathrm{O}_{*,\mathrm{j}} &\xrightarrow{k_r} \quad \mathrm{CO_2(g)} + \quad *_\mathrm{i} + *_\mathrm{j}
\end{aligned}$$

Diffusion Events

$$\begin{aligned}
\mathrm{CO}_{*,\mathrm{i}} + *_\mathrm{j} &\xrightarrow{d_1} \quad *_\mathrm{i} + \mathrm{CO}_{*,\mathrm{j}} \\
\mathrm{O}_{*,\mathrm{i}} + *_\mathrm{j} &\xrightarrow{d_2} \quad *_\mathrm{i} + \quad \mathrm{O}_{*,\mathrm{j}}
\end{aligned}$$

Repulsive CO-CO interactions increase rate constants

Surface Reactions: Points of Interest

- Adsorbate diffusion is fast compared to reaction rates, $\frac{d}{k} \approx O(10^5)$, stops stochastic simulations
- Fast diffusion does NOT mean random particle placement

Fast diffusion with interactions

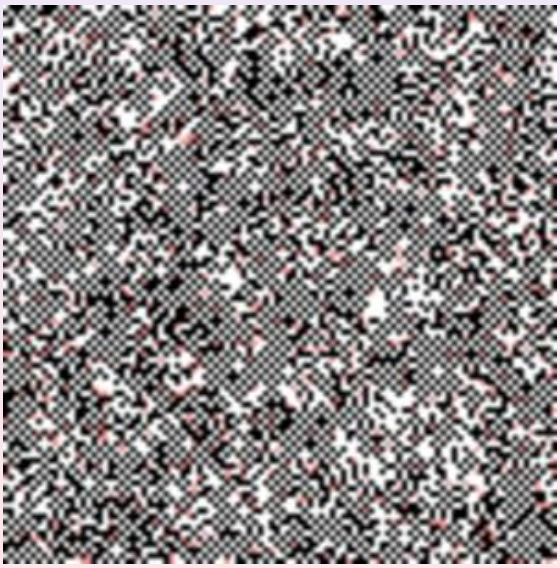

Random particle placement

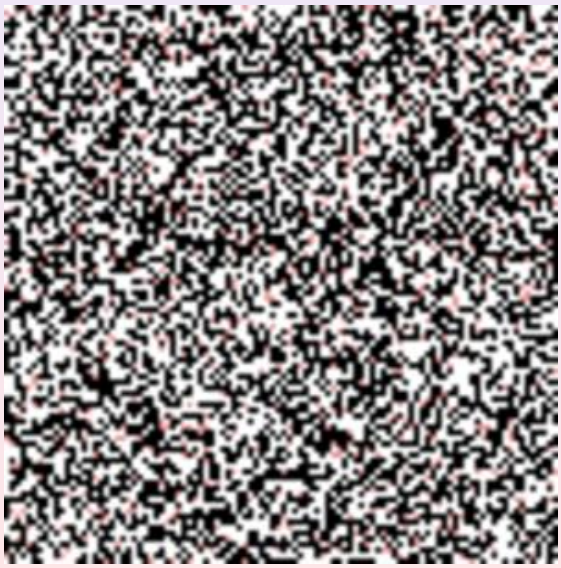

Order Reduction of the Stochastic Master Equation

The chemical master equation

$$\frac{dP(x)}{dt} = \sum_{\beta} W_{x,\beta} P(\beta) - W_{\beta,x} P(x)$$

- For a small (100 sites) lattice the size of the state vector P is $3^{100} \approx 10^{48}$.

Master equation order reduction: fast diffusion limit

- Between reaction events, the lattice samples an equilibrium distribution specified by only species number [6].
- We can show that:

$$\frac{dP(n)}{dt} = \sum_{j} k_j \left[\langle s_j(n-\nu_j) \rangle P(n-\nu_j) - \langle s_j(n) \rangle P(n) \right]$$

- $\langle s_j(n) \rangle$ is the average number of reaction j that can occur given species number n, and is calculated by short diffusion only simulations.
- For a small (100 sites) lattice the size of the state vector P is 5050, solvable linear system.

Surface Reactions: The $\Omega \longrightarrow \infty$ limit

- As the lattice size increases, we switch from a discrete extensive variable n to a continuous intensive variable θ (coverage).
- The reduced master equation can be approximated by an ODE for each species: $\frac{d\theta}{dt} = \sum_{j} k_j \nu_j \langle s_j(\theta) \rangle$

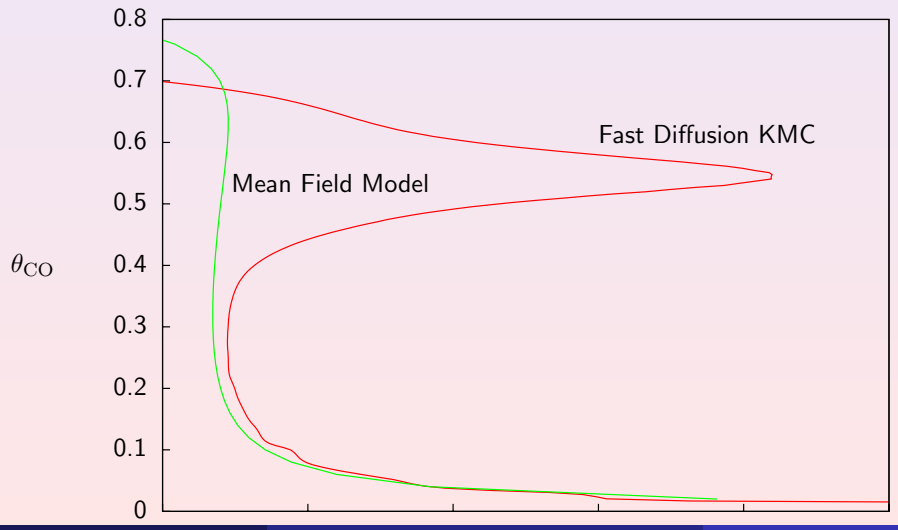

Implications for Crystal Populations

Distributions

Scalars

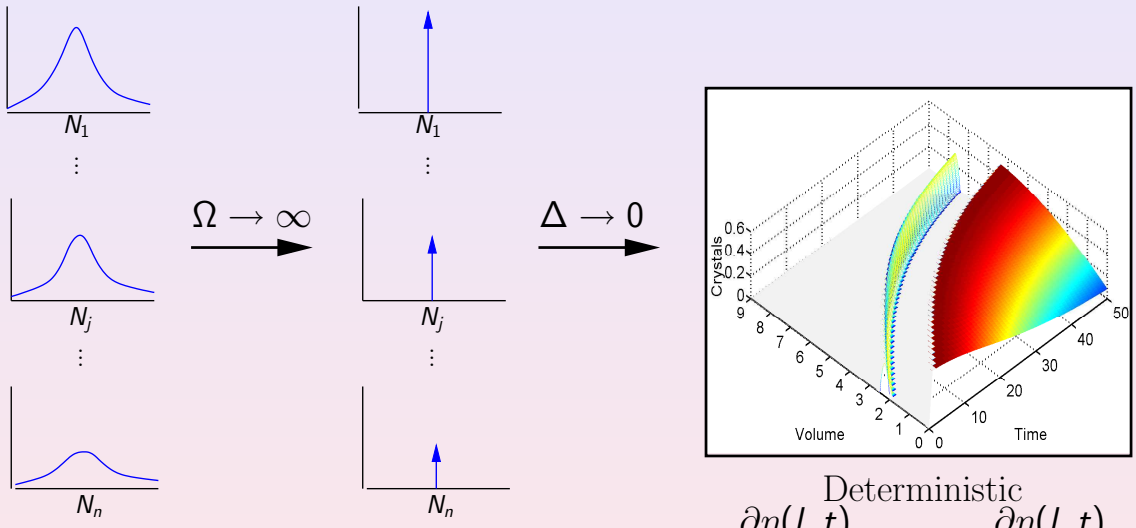

Stochastic

Deterministic

$$\frac{dN_j}{dt} = kM\left(N_{j-1} - N_j\right)$$

Deterministic

$$\frac{\partial \eta(l,t)}{\partial t} = -k'M\frac{\partial \eta(l,t)}{\partial l}$$

Isothermal, Size-Independent Nucleation and Growth

Stochastic Solution

Average of 100 Simulations

Deterministic Solution

Via Orthogonal Collocation

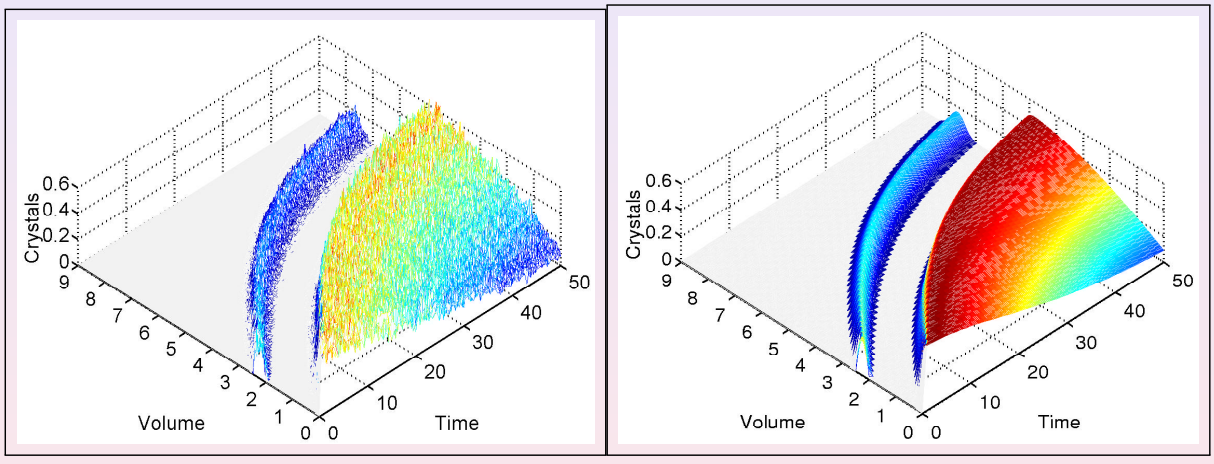

Discrete particle sizes

Integer-valued particle accounting

Continuous particle sizes

Real-valued particle accounting

Nonisothermal, Size-Independent Nucleation and Growth

Stochastic Solution
Average of 500 Simulations

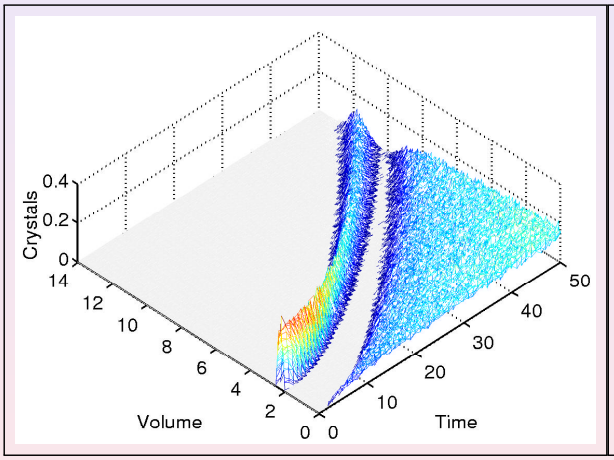

Deterministic Solution
Via Orthogonal Collocation

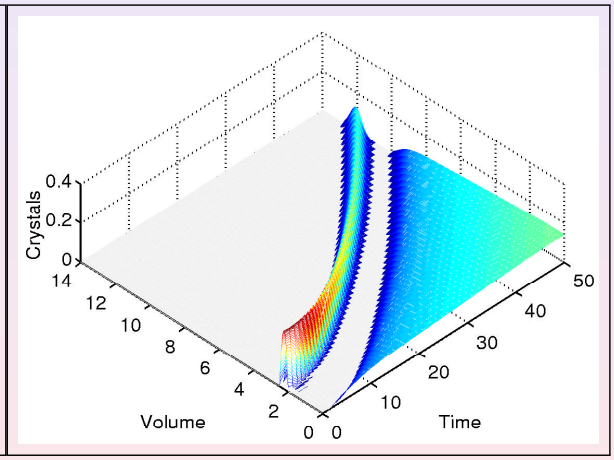

Isothermal, Size-Independent Nucleation, Growth, and Agglomeration

Stochastic Solution

Add one reaction: $N_p + N_q \xrightarrow{k_a} N_{p+q}$
Average of 500 Simulations

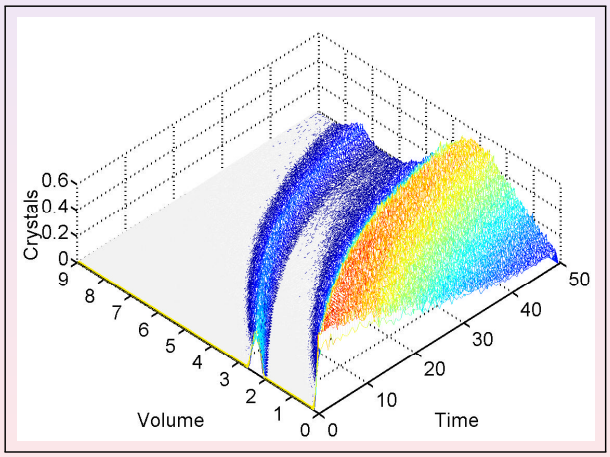

Deterministic Solution

Via Adaptive Mesh Methods?
Large time investment!

Particle shape

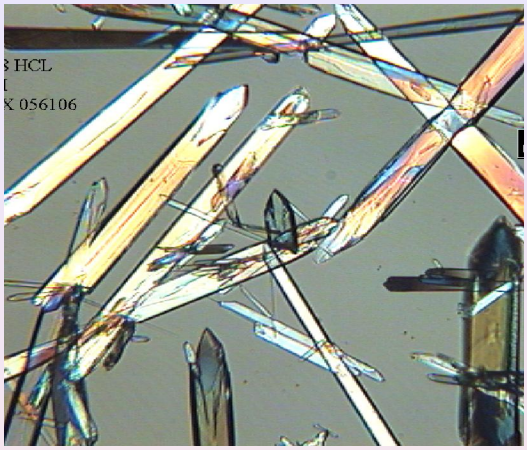

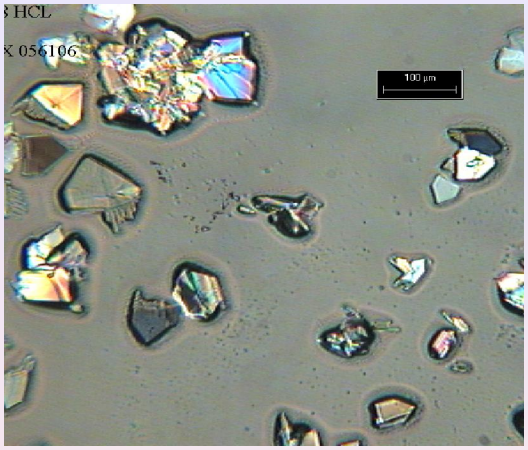

- High value-added products in the chemical industry are becoming increasingly complicated in structure.
- Pharmaceutical compounds are very complex: multiple crystal habits and multiple crystal structures.

Particle shape—industrial characteristics and challenges

- Particle shape is affected by unmeasured disturbance variables that cannot be modeled nor controlled.
- Online sensing is available in the form of video images. The images are replete with bad data.
  - Particles are fused or broken; particle boundaries overlap.
  - It is difficult to obtain representative samples.
  - It is difficult to sample enough images to remove the effects of noise through averaging.
- Standard image analysis software provides simple shape measures such as particle boxed area and aspect ratio. These simple measures are inadequate signals for feedback control.

Macroscopic sodium chlorate ($NaClO_3$) habit

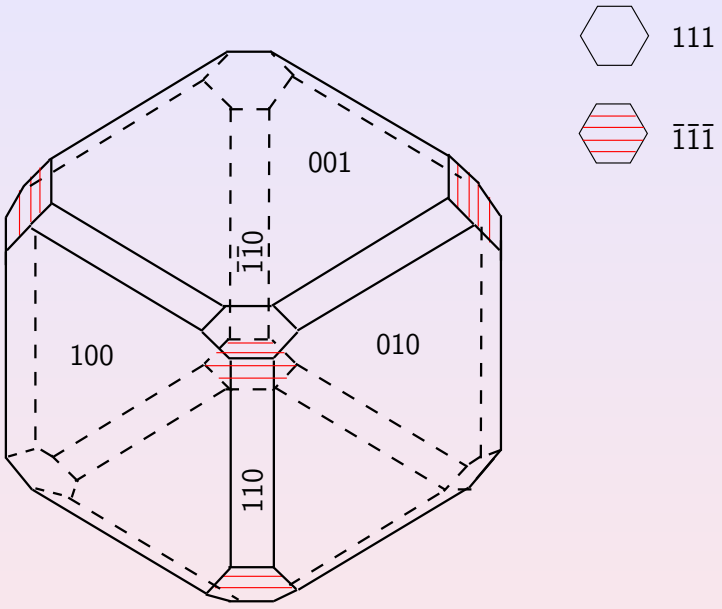

- The 110, 111 and $\bar{1}\bar{1}\bar{1}$ faces grow fast under relatively high supersaturation and "grow out" leaving only the 100 faces visible under microscopy.

Macroscopic sodium chlorate ($NaClO_3$) habit

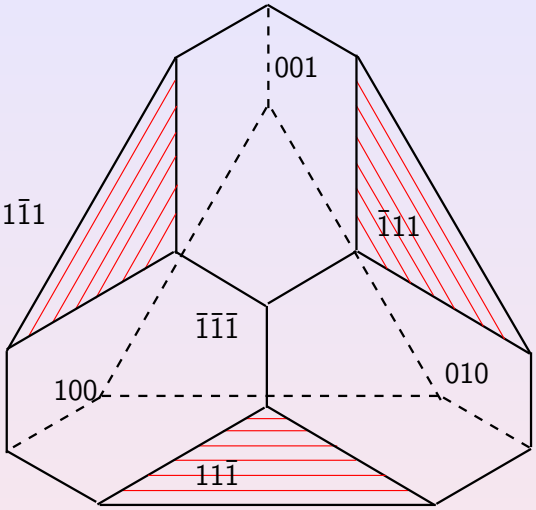

- In the presence of sodium dithionate ($Na_2S_2O_6$) the $\bar{1}\bar{1}\bar{1}$ faces are blocked by the impurity and the 100, 110 and 111 faces grow relatively faster, leaving only the $\bar{1}\bar{1}\bar{1}$ faces visible, seen as a tetrahedron under microscopy.
- See Sherwood, Ristic, and coworkers for further discussion [16, 15]

Experimental apparatus

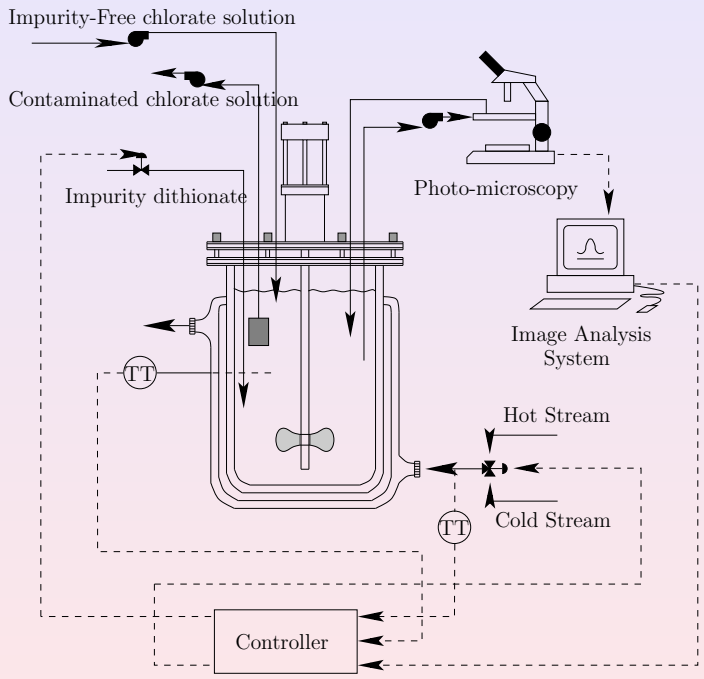

- Cascaded MPC-PI temperature controller.
- Automated image analysis system provides on-line information about particle size and shape by binarizing images of samples of the crystal slurry.

Sodium chlorate shape manipulation

Figure i 15 min
no habit modifier

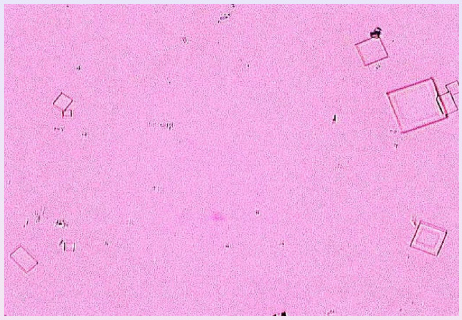

200μm

Figure ii 49 min
225ppm $Na_2S_2O_6$

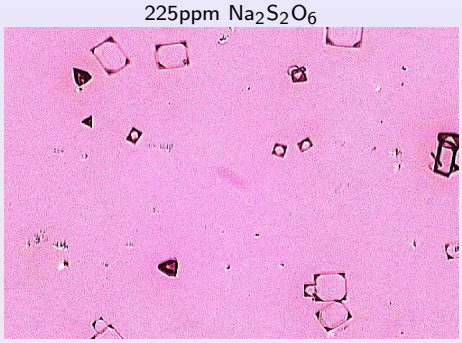

200μm

Figure iii 70 min
225ppm $Na_2S_2O_6$

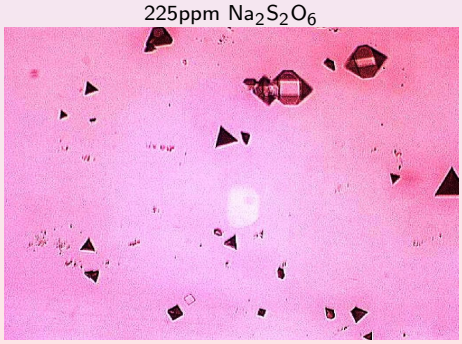

200μm

Figure iv 135 min
no habit modifier

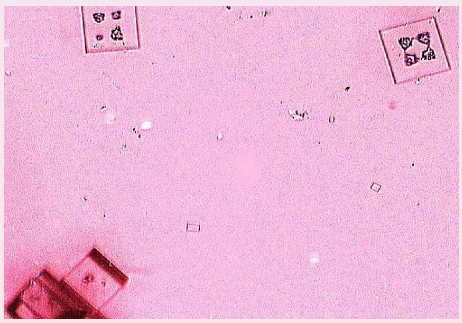

200μm

Perturbations to squares and equilateral triangles

		square	triangle
aspect ratio	$\frac{L_{max}}{L_{min}}$	$\sqrt{2}$	$\frac{3\sqrt{3}}{4}$
roundness	$\frac{per^2}{4\pi area}$	$\frac{4}{\pi}$	$\frac{9}{\pi\sqrt{3}}$
boxed area	$\frac{\text{object area}}{\text{bounding box area}}$	1.0	0.5

- Saw tooth waves of increasing amplitude are added to the boundaries of a square and triangle and sized to assess the reliability of the sensor.

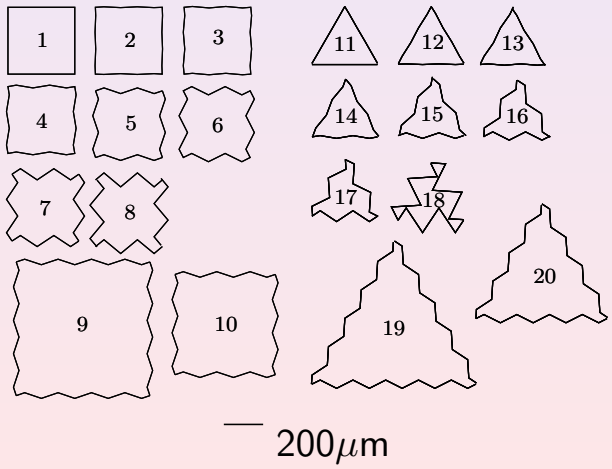

Classification of shape

- The size of the elliptical regions is chosen to classify the shapes.
- Only data within the elliptical regions are used.

Classification regions

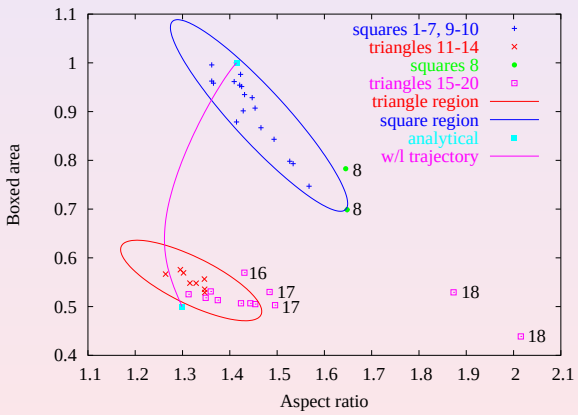

Classification regions and data

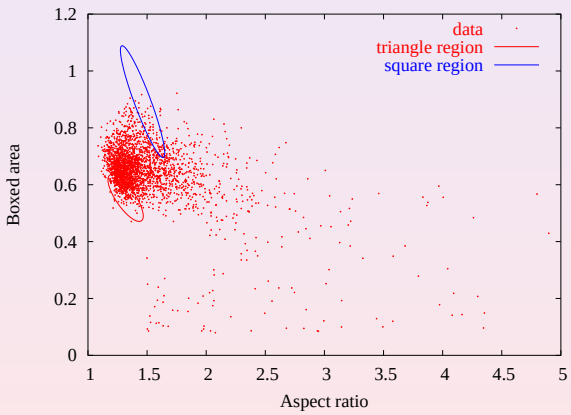

Processed image data

- Sensor detects clearly shape change using square and triangle regions alone.

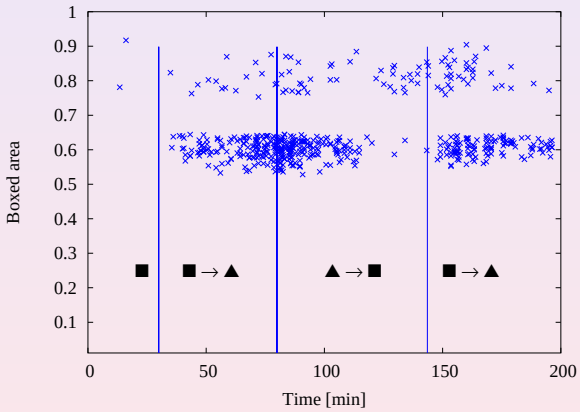

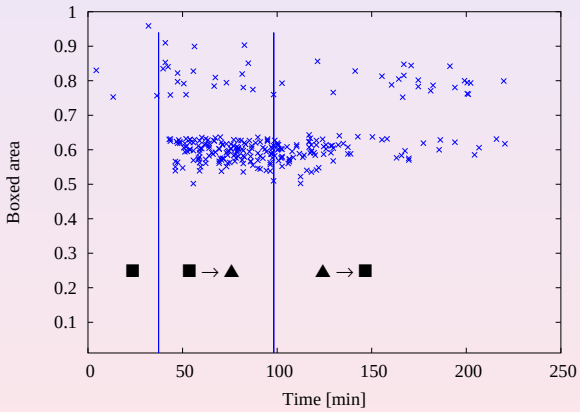

Feedback control of particle shape to steady state

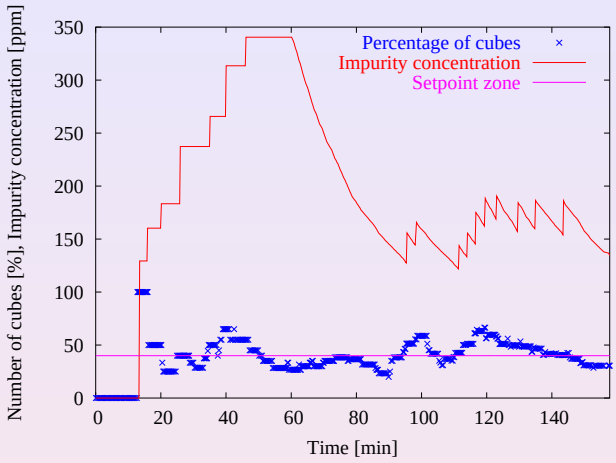

- By maintaining the habit modifier at a level near the critical impurity concentration, simple PI control algorithms are able to keep a desired habit in the presence of a disturbance. The controller finds the critical dosage (140-160 ppm) required to achieve 40% cubes in a slurry without any knowledge of a model. This value agrees with literature values of 50-210 ppm (Sherwood 1993).

Limitations of current vision-based measurements

- Commercial, vision-based particle characterization instruments require sampling.
- Literature methods are inadequate for typical industrial, in situ images[1]

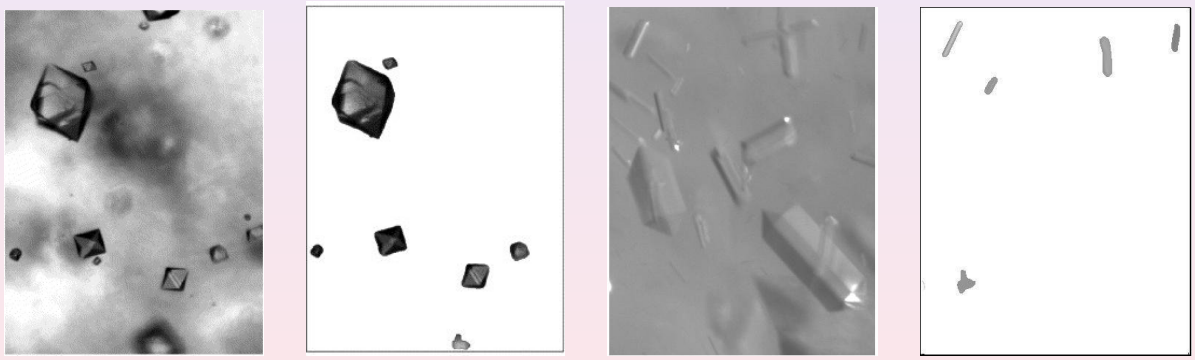

[1] Calderon De Anda et. al., *Chemical Engineering Science*, 2005.

Model-based object recognition for shape measurement

Advantages

1. Parallel, distributed algorithms.
2. Robust to noise or missing data.
3. Generalizable to many shapes.

Basic approach[2]

1. Find linear features in the image.
2. Find linear feature clusters that appear significant on the basis of viewpoint-independent relationships (collinearity, parallelism, and end-point proximity).
3. Fit a two or three-dimensional model to each line cluster.

[2] Lowe, D.G., *Artificial Intelligence*, 1987.

2-D model-based image analysis for needles

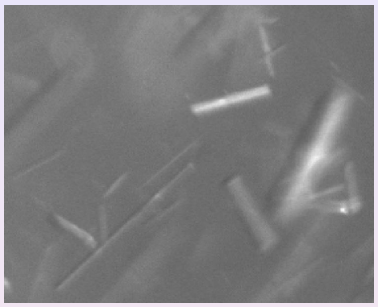

Original image

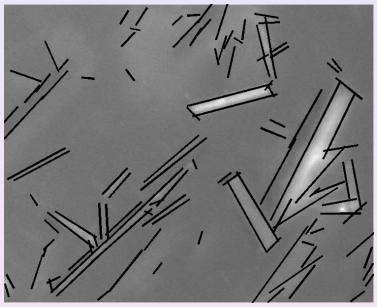

Linear feature detection

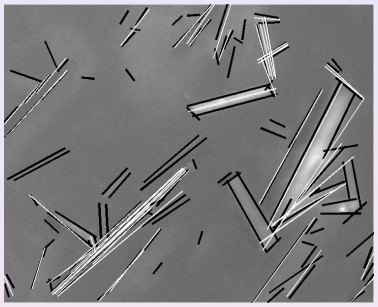

Collinearity identification

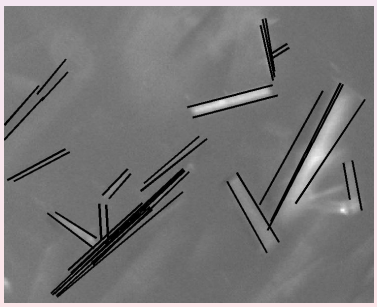

Parallelism identification

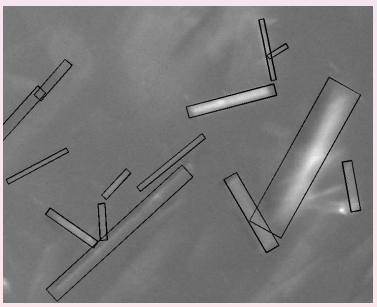

Cluster properties

Results for pharmaceutical crystallization

Time = 85 min. after seeding, Temp. = 44 deg. C

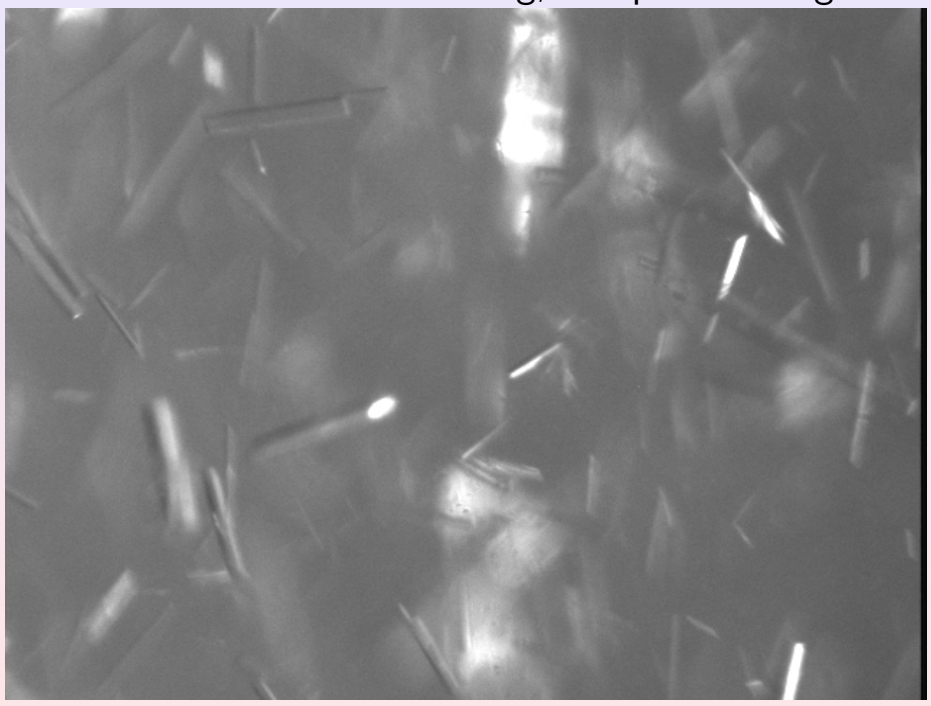

Results for pharmaceutical crystallization

Time = 85 min. after seeding, Temp. = 44 deg. C

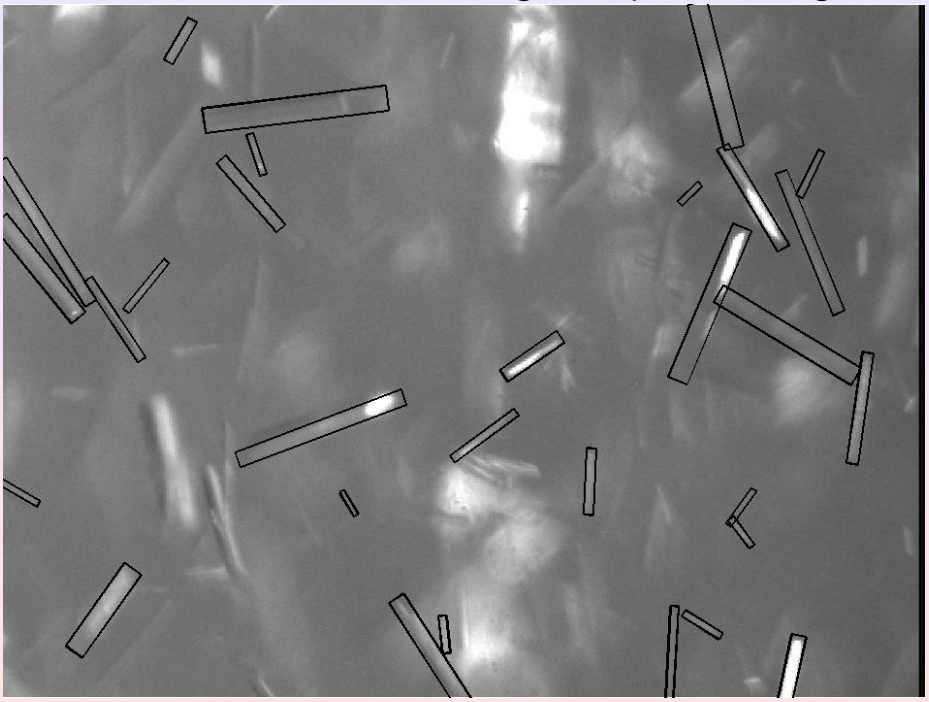

Results for pharmaceutical crystallization

Time = 265 min. after seeding, Temp. = 20 deg. C

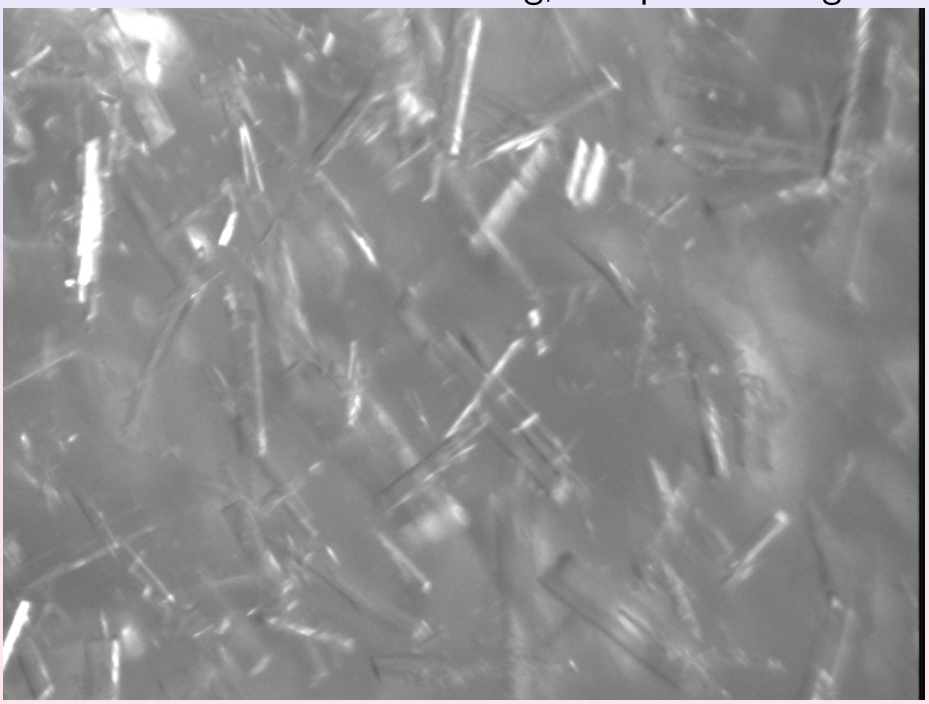

Results for pharmaceutical crystallization

Time = 265 min. after seeding, Temp. = 20 deg. C

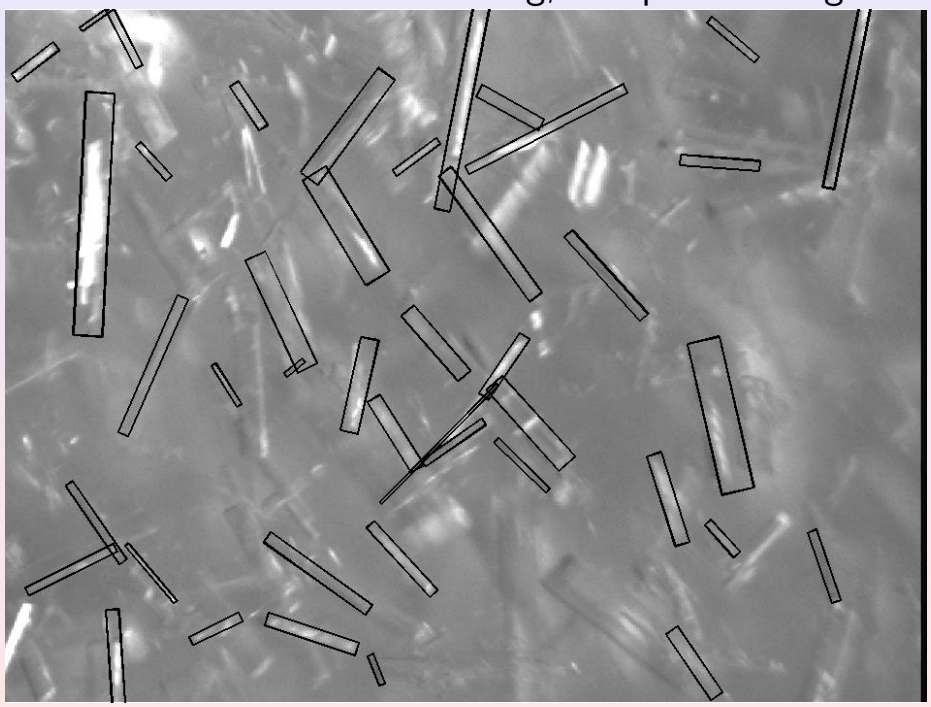

Comparison of automatic and manual measurement

Time (min.)	Temp. (deg C)	Mean Size, (μm) Manual	Automatic	Percent Difference
85	44	284	300	5.5
125	41	291	292	0.4
210	30	288	286	0.7
265	20	356	303	14.8

85 min., 44 deg C

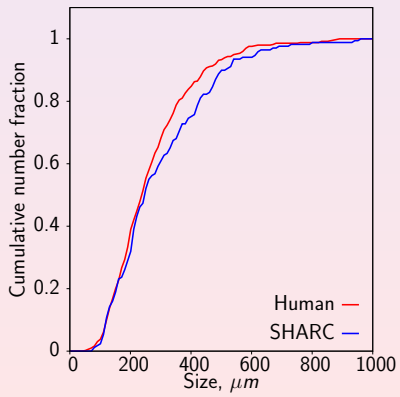

210 min., 30 deg C

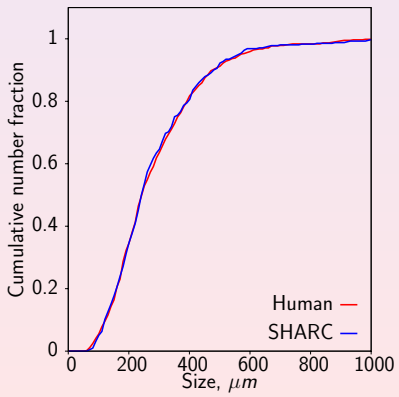

265 min., 20 deg C

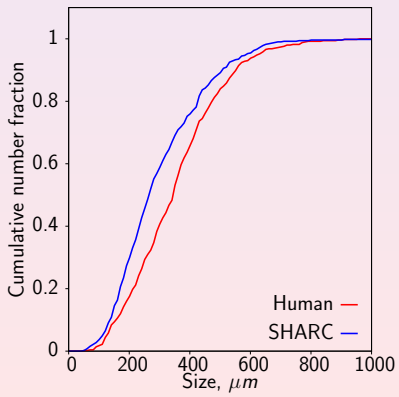

3-D models for more complex shapes

- Parameterized, wireframe model.
- Viewpoint-invariant groups used as cues for location and size of crystals in image.

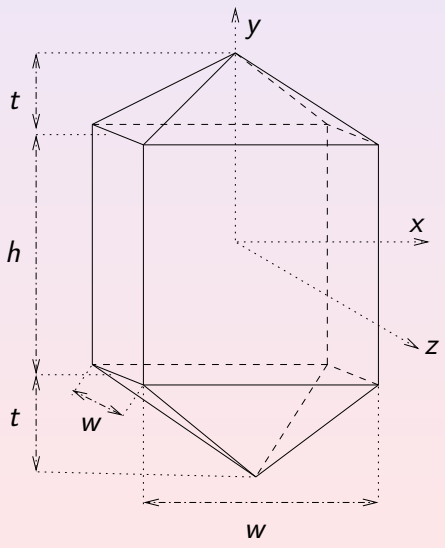

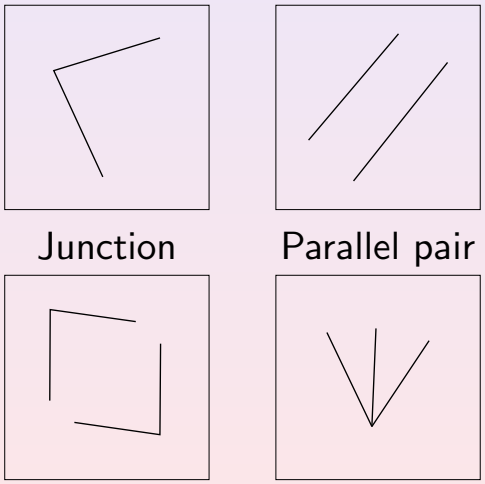

Application to in situ image

Algorithm steps:

- Identify linear features in image.
- Identify significant, viewpoint-invariant groups.
- Use the location, orientation, and lengths of the lines in the group to estimate the crystal's size and orientation.

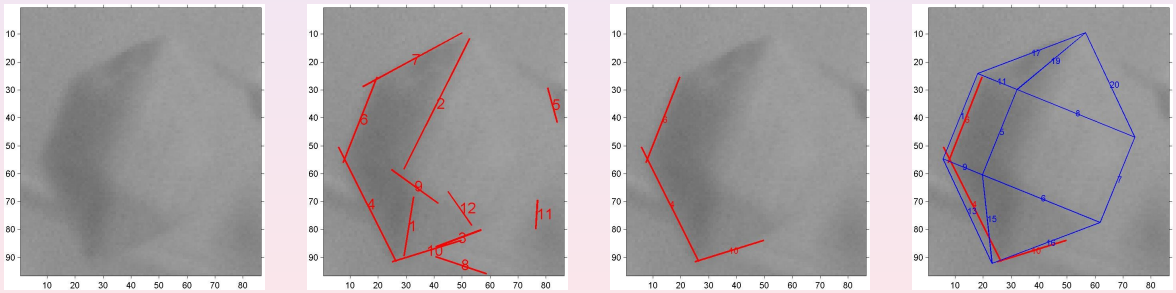

Example 1: α-glycine crystal

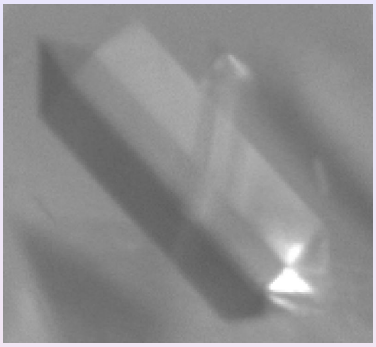

(a) Original image

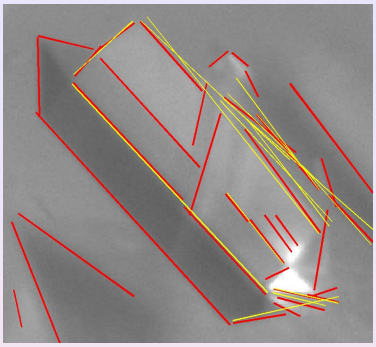

(b) Linear features

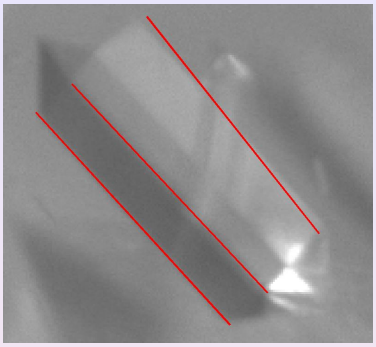

(c) Salient line group

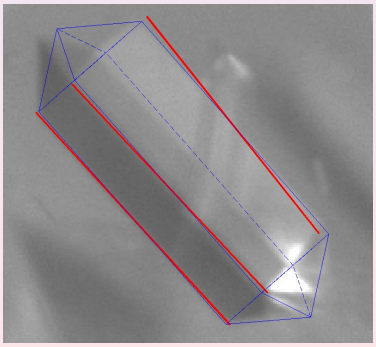

(d) Model initialization

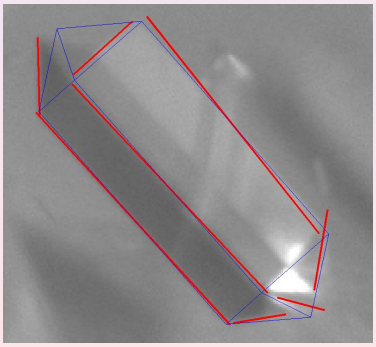

(e) Further matches

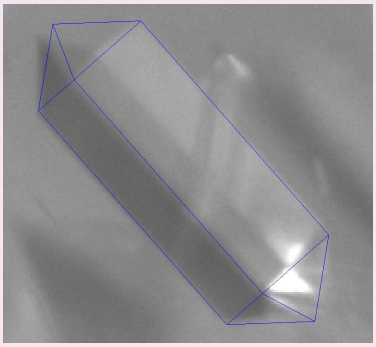

(f) Optimized Fit

Example 2: γ-glycine crystal

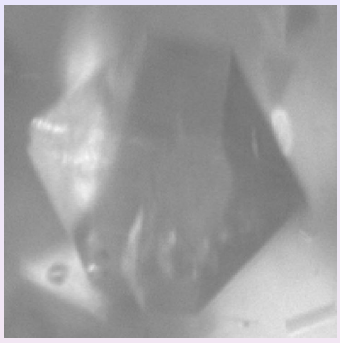

(a) Original image

(b) Linear features

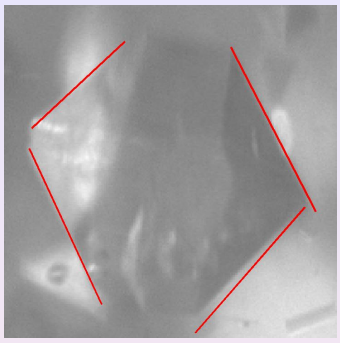

(c) Salient line group

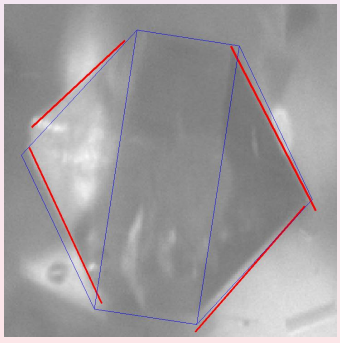

(d) Model initialization

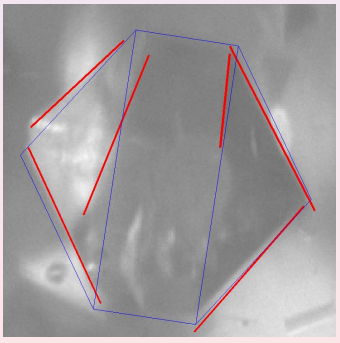

(e) Further matches

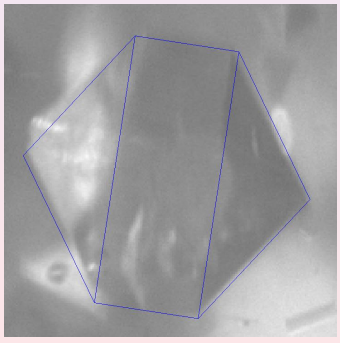

(f) Optimized Fit

Application to full image: α-glycine

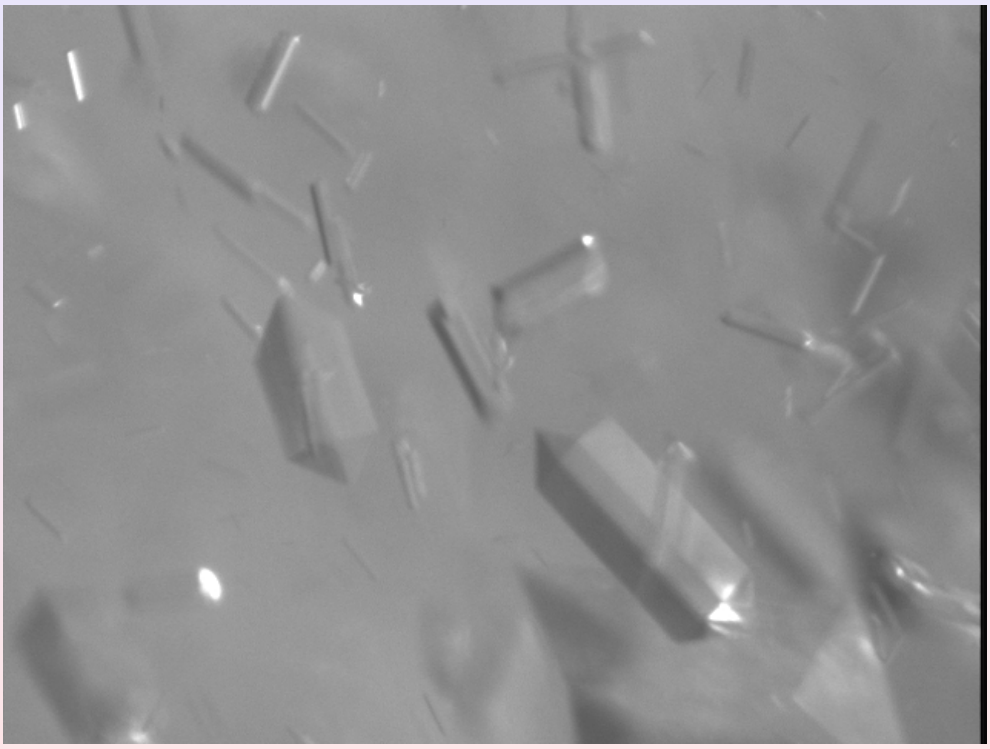

Application to full image: α-glycine

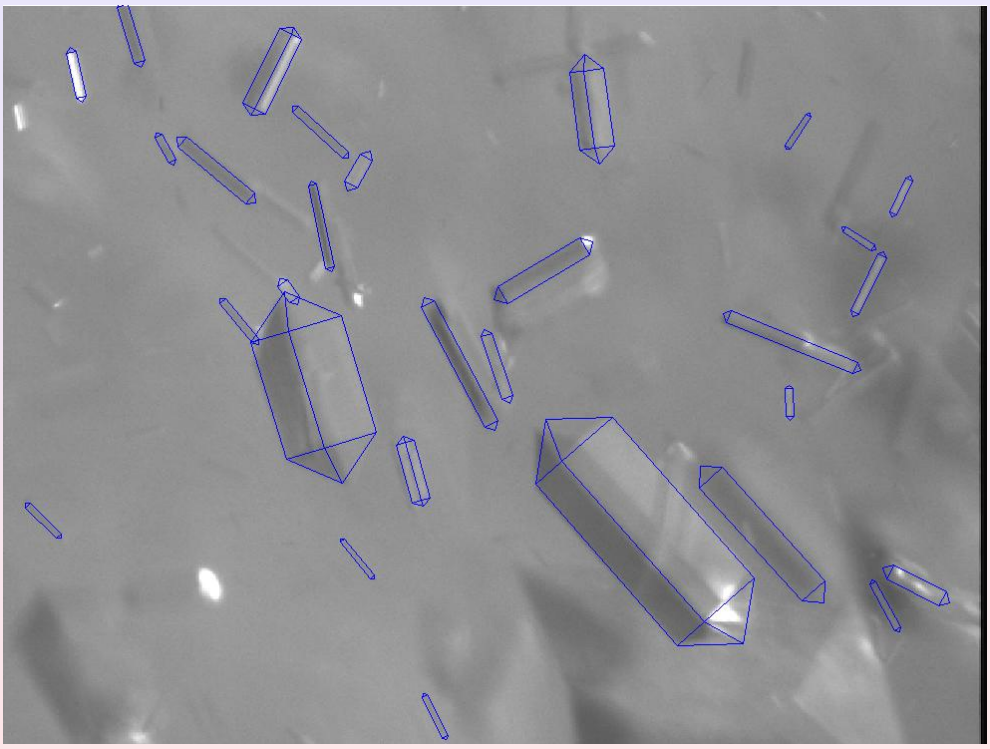

Application to full image: γ-glycine

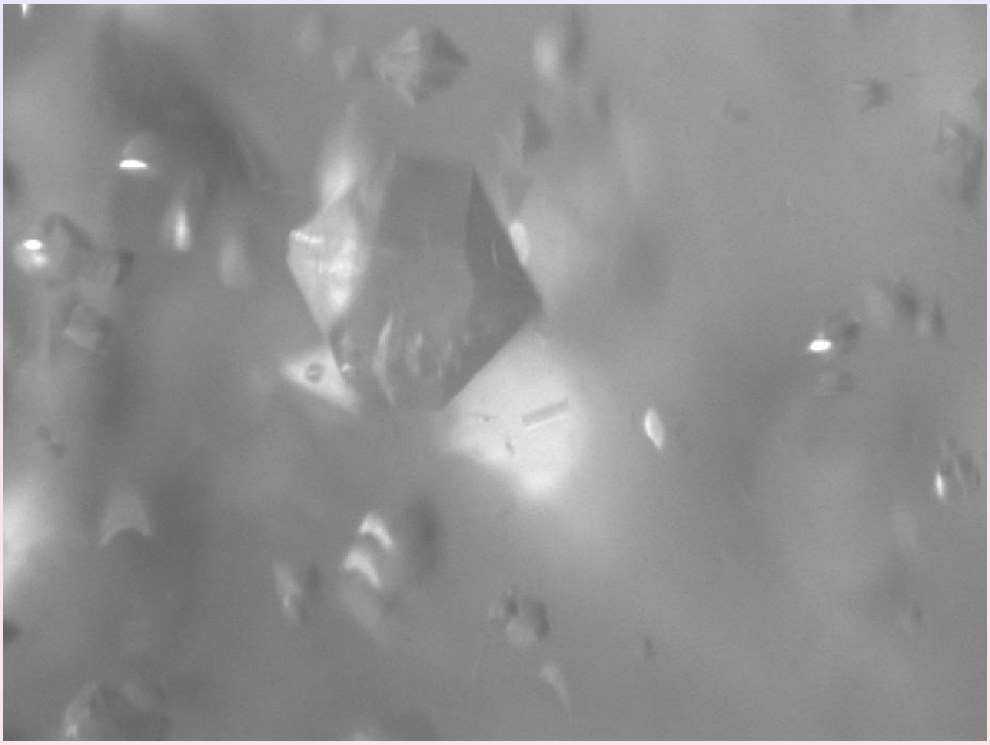

Application to full image: γ-glycine

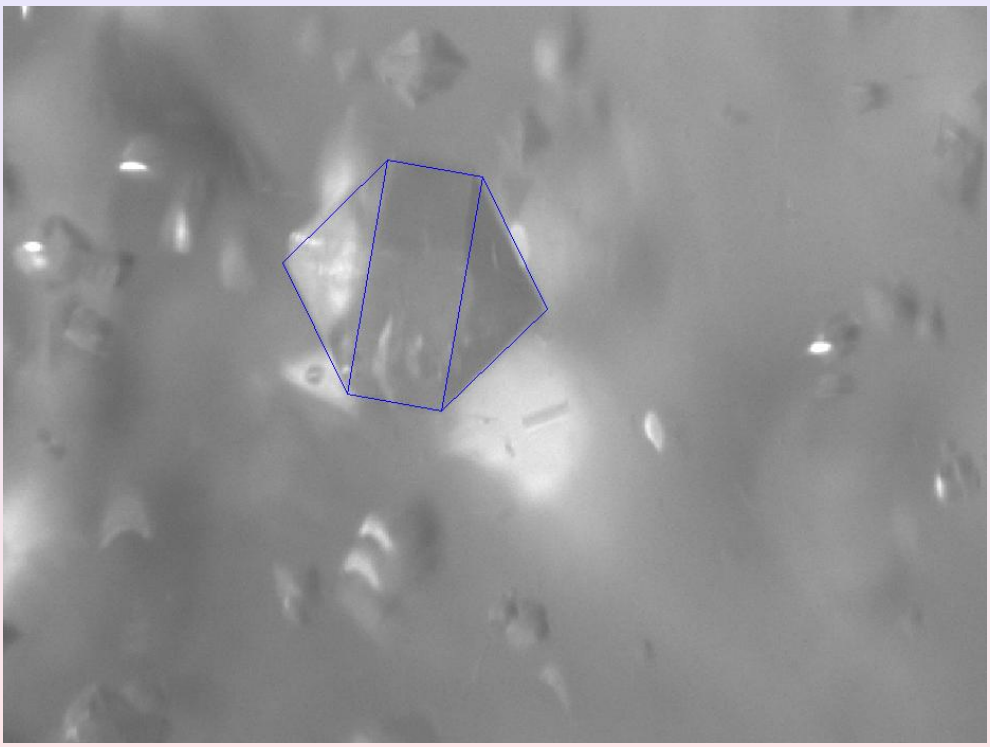

Conclusions

- If you want to understand data . . . you have to model them
- Good models enable good engineering: design, monitor, forecast, control
- Crystal engineering poses challenging modeling problems, but progress is steady and breakthroughs are possible
  - off-the-shelf data/model combinations are *often* incompatible
  - these applications require state-of-the-art modeling tools for numerical solution, parameter estimation, optimization and control
- We are capable of modeling, monitoring and controlling many systems with current technology

Measurement Technology

- Model-based vision is a promising method for automating the measurement of crystal size and shape distributions in noisy, in situ images.
- Both needle and template-based algorithms have been developed and applied for specific shapes. The needle algorithm achieves results roughly as good as those obtained from manual sizing of crystals. Further validation is needed for the template algorithm.
- The algorithms are fast and likely suitable for real-time measurement of crystal size and shape distributions and polymorphic composition.

Looking to the future: multiscale modeling

- More and better sensors
  - in-situ video imaging for on-line particle analysis appears feasible
  - commercial instrument vendors are very active
  - complex product specifications require better sensors
- More and better models
  - couple ab initio molecular, chemical models to process models
  - move from simple scaling heuristics to mixing models based on computational fluid dynamics
  - real-time compression of large sets of video data into useful information
  - stochastic simulation of complex population behavior

Acknowledgments

Ph.D. Students and Postdocs

- Paul A. Larsen and Ethan A. Mastny
- Eric L. Haseltine (graduated 2/2005)
- Daniel B. Patience (graduated 8/2002)

Funding

- GlaxoSmithKline
- Mitsubishi Chemical
- International Fine Particle Research Institute (IFPRI)
- Amoco
- National Science Foundation

Further Reading I

[1] T. Allen. *Particle Size Measurement*. Chapman and Hall, London, fifth edition, 1997.

[2] M. H. Bharati and J. F. MacGregor. Multivariate image analysis for real-time process monitoring and control. *Ind. Eng. Chem. Res.*, 37:4715–4724, 1998.

[3] R. D. Braatz and S. Hasebe. Particle size and shape control in crystallization processes. In *Chemical Process Control—CPC 6*, pages 307–327, Tucson, Arizona, January 2001.

[4] D. T. Gillespie. A general method for numerically simulating the stochastic time evolution of coupled chemical reactions. *J. Comput. Phys.*, 22:403–434, 1976.

[5] D. T. Gillespie. Exact stochastic simulation of coupled chemical reactions. *J. Phys. Chem.*, 81:2340–2361, 1977.

[6] E. L. Haseltine and J. B. Rawlings. On the origins of approximations for stochastic chemical kinetics. *J. Chem. Phys.*, 123:164115, October 2005.

[7] C. M. G. Heffels, D. Heitzmann, E. D. Hirleman, and B. Scarlett. The use of azimuthal intensity variations in diffraction patterns for particle shape characterization. *Part. Part. Syst. Charact.*, 11:194–199, 1994.

Further Reading II

[8] C. M. G. Heffels, D. Heitzmann, E. D. Hirleman, and B. Scarlett. Forward light scattering for arbitrary sharp-edged convex crystals in Fraunhoffer and anomalous diffraction approximations. *Applied Opt.*, 34(26):6552–6560, 1995.

[9] H. B. Matthews and J. B. Rawlings. Batch crystallization of a photochemical: Modeling, control and filtration. *AIChE J.*, 44:1119–1127, 1998.

[10] O. Monnier, G. Fevotte, C. Hoff, and J. P. Klein. Model identification of batch cooling crystallizations through calorimetry and image analysis. *Chem. Eng. Sci.*, 52(7):1125–1139, 1997.

[11] D. B. Patience, H. A. Mohameed, and J. B. Rawlings. Crystallization of para-xylene in scraped-surface crystallizers. *AIChE J.*, 47(11):2441–2451, 2001.

[12] D. B. Patience and J. B. Rawlings. Particle-shape monitoring and control in crystallization processes. *AIChE J.*, 47(9):2125–2130, 2001.

[13] C. J. G. Plummer and H. H. Kausch. Real-time image analysis and numerical simulation of isothermal spherulite nucleation and growth in polyoxymethylene. *Colloid Polym. Sci.*, 273:719–732, 1995.

[14] J. B. Rawlings, S. M. Miller, and W. R. Witkowski. Model identification and control of solution crystallization processes: A review. *Ind. Eng. Chem. Res.*, 32(7):1275–1296, July 1993.

Further Reading III

[15] R. Ristić, B. Y. Shekunov, and J. N. Sherwood. Growth of the tetrahedral faces of sodium chlorate crystals in the presence of dithionate impurity. *J. Cryst. Growth*, 139(3-4):336–343, 1994.

[16] R. Ristić, J. N. Sherwood, and K. Wojciechowski. Morphology and growth kinetics of large sodium chlorate crystals grown in the presence and absence of sodium dithionate impurity. *J. Phys. Chem.*, 97(41):10774–10782, 1993.

[17] R. D. Rovang and A. D. Randolph. On-line particle size analysis in the fines loop of a KCl crystallizer. *AIChE Symp. Ser.*, 76(193):798–807, 1980.

[18] B. H. Shah, D. Ramkrishna, and J. D. Borwanker. Simulation of particulate systems using the concept of the interval of quiescence. *AIChE J.*, 23(6):897–904, 1977.

[19] H. C. van de Hulst. *Light Scattering by Small Particles*. Dover Publications, New York, 1981.